CDF/ANAL/EXOTIC/CDFR/5570
version 1.0, Ferbrary 26, 2001
version 2.0, March 12, 2001
version 3.0, June 14, 2001
version 4.0, February 11,2003
version 4.5, April 22, 2003

Search for R-Parity Violating Decays of Scalar Top Quarks in Two Taus and Two Jets Events — Electron Channel —

Y. Miyazaki,[a] M.J. Kim,[b] M. Tanaka,[c] T. Kamon,[d]
M. Chertok,[e] J.P. Done,[d] Y. Kato,[a]
D.H. Kim,[f] T. Okusawa,[a] Y. Seiya,[c] and K. Yamamoto,[a]
(a) Osaka City Universit, (b) Carnegie Mellon University,
(c) University of Tsukuba, (d) Texas A&M University,
(e) University of California, Davis
(f) Korean Center for High Energy Physics,

Abstract

We search for the scalar top quark pair production ($\tilde{t}_1\bar{\tilde{t}}_1$) in which $\tilde{t}_1$ decays via the R-parity violating ($\not{R}_p$) process using data collected by the CDF detector during 1992–1995 in $p\overline{p}$ collisions at $\sqrt{s}$ = 1.8 TeV. The R-parity is a quantum number which distinguishes between Standard Model particles and supersymmetric particles. We assume the R-parity is only violated in the third generation and $\tilde{t}_1$ decays into $\tau^+\overline{b}$. Our experimental signature is one lepton(e or μ) decaying from a tau lepton, one hadronically decaying tau lepton(τ_h), and two jets. We report the analysis for the electron channel. The number of events that passed our selection in the data (106 pb^{-1}) is found to be zero, where the number of backgrounds expected from the Standard Model processes is 1.97 $^{+1.01}_{-0.11}$ (stat) $\pm$ 0.15 (sys). We set a lower limit on the $\tilde{t}_1$ mass at 110 GeV/c^2 at 95 % confidence level.

1 Introduction

1.1 Supersymmetry

The predictions from Standard Model (SM) are in quite good agreement with the experimental measurements up to date. However, SM has several problems which cannot be solved without the introduction of new physics. Supersymmetry (SUSY) [1] is one of the candidates for the new physics, which introduces symmetry between fermions and bosons. By assuming a symmetry between fermions and bosons, it becomes possible to solve the problem of quadratic divergence and explain the hierarchy between the electroweak mass scale and the Plank mass scale. SUSY introduces supersymmetric particles each of which is a superpartner of SM particles. Supersymmetric particles have a spin which is a half-unit different with that of SM particles. Most of the works in the SUSY searches are being performed within the Minimal Supersymmetric extension of the Standard Model (MSSM) [2].

1.2 R-parity

MSSM introduces a new quantum number which distinguishes between SM particles and Supersymmetric particles. The new quantum number is called R-parity (R_p), which is defined as

$$R_p \equiv (-1)^{3B+L+2S}, \tag{1}$$

where B is the baryon number, L is the lepton number, and S refers to the spin. R_p represents $+1$ for SM particles and -1 for supersymmetric particles. If the R-parity is conserved, supersymmetric particles are always produced in pairs and decay through a cascade to SM particles and the lightest supersymmetric particles (LSP). This process involves large missing energy as its signature. However, the R-parity conservation is not ensured by the gauge invariance and there is no reason to forbid the R-parity violation ($\not{R}_p$). The R-parity violation introduces the lepton and baryon number violation.

A superpotential is given by

$$W = W_{MSSM} + W_{\not{R}_p}, \tag{2}$$

where W_{MSSM} is the superpotential term of MSSM which conserves the R-parity, while $W_{\not{R}_p}$ is the superpotential term which violates the R-parity. W_{MSSM} is given by

$$W_{MSSM} = \varepsilon_{ij}\mu \hat{H}_u^i \hat{H}_d^j + \epsilon_{ij}\left[\lambda_L \hat{H}_u^i \hat{L}^j \hat{E}^c + \lambda_D \hat{H}_u^i \hat{Q}^j \hat{D}^c + \lambda_U \hat{H}_d^i \hat{Q}^j \hat{U}^c\right], \tag{3}$$

where i and j are the SU(2) indices, μ is the Higgs mass parameter, $\hat{H}_{u(d)}$ is the Higgs doublet. $\hat{L}$ and $\hat{Q}$ are the left-handed doublets of leptons and quarks, while $\hat{E}^c$, $\hat{D}^c$, and $\hat{U}^c$ are the right-handed singles of charged leptons, down-type and up-type quarks, respectively. λ could be all matrices which mix the interaction of the three generations.

$W_{\not R_p}$ has of two-types of R-parity violating terms. One includes the explicit R-parity violation resulting from the trilinear $\not R_p$ (TRPV) couplings and the other includes the spontaneous R-parity violation resulting from the bilinear $\not R_p$ (BRPV) couplings. Namely, $W_{\not R_p}$ is written by

$$W_{\not R_p} = W_{TRPV} + W_{BRPV}, \tag{4}$$

where W_{TRPV} and W_{BRPV} represent the superpotentials for the trilinear and bilinear $\not R_p$ couplings respectively. W_{TRPV} is given by

$$W_{TRPV} = \varepsilon_{ij} \left[\lambda_{ijk} \hat{L}^i \hat{L}^j \hat{E}^{ck} + \lambda^{'}_{ijk} \hat{L}^i \hat{Q}^j \hat{D}^{ck} + \lambda^{''}_{ijk} \hat{U}^{ci} \hat{D}^{cj} \hat{D}^{ck} \right], \tag{5}$$

and W_{BRPV} is given by

$$W_{BRPV} = \varepsilon_{ij} \epsilon_i \hat{L}^i \hat{H}^j_d, \tag{6}$$

where ϵ_i is the coupling of the lepton number violation in the i-th generation.

In the TRPV framework, the lepton number violation is induced by the λ_{ijk} and $\lambda^{'}_{ijk}$ terms, while the baryon number violation is induced by the $\lambda^{''}_{ijk}$ terms [3]. λ_{ijk} is antisymmetric under the interchange of the first two indices, while $\lambda^{''}_{ijk}$ is antisymmetric under the interchange of the last two. Thus, there are 27 free parameters for $\lambda^{'}$ and 9 for λ and $\lambda^{''}$. Namely, the TRPV involves 45 free parameters in total.

On the other hand, in the BRPV framework, the R-parity is spontaneously broken through the vacuum expectation values (VEV) of the right-handed sneutrinos $<\tilde{\nu}>= v_R \neq 0$ [4]. The ϵ_3 parameter induces a non-zero VEV of the left-handed tau neutrinos $<\tilde{\nu}>= v_3/\sqrt{2}$. v_3 contributes to the W mass according to $m_W^2 = \frac{1}{4} g^2 (v_u^2 + v_d^2 + v_3^2)$, where v_u and v_d are the VEV's of the Higgs doublets. In introducing the BRPV, charginos mix with charged leptons, neutralinos mix with neutrinos, and charged sleptons mix with charged Higgs bosons.

We focus on the lightest scalar top quark (stop or $\tilde{t}_1$) because the stop could be the lightest or the next lightest supersymmetric particle (LSP or NLSP). Assuming that the R-parity violation only happens in the third generation, the stop can decay into a tau lepton and a bottom quark by violating the R-parity as follows:

$$\tilde{t}_1 \rightarrow \tau^+ + b. \qquad \text{(Channel 1)}$$

This decay channel is possible in both TRPV ($\lambda^{'}_{333}$) and BRPV (ϵ_3). The branching ratio of this channel will be 100 % in both frameworks if the stop is the LSP. If the LSP is the lightest neutralino ($\tilde{\chi}^0_1$) with the NLSP being the stop, the stop can decay into $\tilde{\chi}^0_1$ and a charm quark with the R-parity conservation.

$$\tilde{t}_1 \rightarrow \tilde{\chi}^0_1 + c \qquad \text{(Channel 2)}$$

However, if $|\epsilon_3|$ and $|v_3|$ are below a GeV, it is possible that the decay mode of the stop shown in Channel 1 is dominant in the BRPV even when the LSP is $\tilde{\chi}^0_1$ [5].

Therefore, the Channel 1 is important for a signature of the R-parity violation. We search for evidence of the direct production of stop pairs followed by $\tilde{t}_1(\bar{\tilde{t}}_1)$ decay into a tau lepton and a bottom quark as follows:

$$p\bar{p} \to \tilde{t}_1\bar{\tilde{t}}_1 + X \to \tau^+ + b + \tau^- + \bar{b} + X.$$

The most recent and competing result on the mass limit in the same $\not{R}_p$ scenario is from the ALEPH experiment [6]. The limit is set at 93 GeV/c^2 in $e^+e^- \to \tilde{t}_1\bar{\tilde{t}}_1 \to \tau^+\tau^- +$ 2-jets with an assumption of $\lambda'_{33k} \neq 0$ ($k = 1$, 2, or 3).

This note is organized as follows. We first describe the overview of CDF note 5251[7] on the $Z \to \tau\tau$ event analysis in Section 2. In Section 3, we discuss the method to determine the stop pair production cross section by normalizing with the $Z \to \tau\tau$ events. Section 4 describes the dataset and baseline sections for our analysis. In Section 5 shows the studies of backgrounds for our analysis. Then, we show studies of $Z \to \tau\tau$, $\tilde{t}_1\bar{\tilde{t}}_1 \to \tau b\tau\bar{b}$ and systematic uncertainties in Section 6, 7 and 8, respectively. Finally, we show the results and conclusions of this analysis in Section 9 and 10, respectively. We report the analysis for electron channel in this note.

2 Overview of CDF 5251

We studied $Z \to \tau\tau$ events with a central lepton ($\ell = e$ or μ) with $p_T(\ell) \geq 10$ GeV/c and a hadronically decaying τ (τ_h) with $p_T(\tau_h) \geq 15$ GeV/c from the Run IB low p_T lepton trigger datasets [7]. In order to improve the acceptance for $Z \to \tau\tau$ events compared to the two previous studies [8, 9], we made two major changes in our analysis:

(i) Lowering the p_T threshold for leptons from 20 GeV/c to 10 GeV/c.

(ii) Using a τ_h identification code based on track, used in the top dilepton ($\ell + \tau_h$) analysis [10], which includes π^0 reconstruction [11].

After the baseline selection, the dominant sources of the $\ell + \tau_h$ events were found to be $Z \to \tau\tau$, W + jets, and QCD events. For rejection of these background processes, we applied the following two cuts:

(i) $M_T(\ell, \not{E}_T) \leq 25$ GeV/c^2 for $W +$jets rejection

(ii) $|\vec{E}_T(\ell) + \vec{\not{E}}_T| \geq 25$ GeV/c for QCD event rejection

Table 1 shows the summary of $Z \to \tau\tau$ event candidates of an isolated electron/muon (ℓ) and a hadronically decaying tau lepton (τ_h). In the above analysis, we took the known efficiencies (trigger efficiencies, lepton ID and isolation efficiencies) into account in the MC samples. However, we see a difference of the number of events between the data and MC. This reason is considered to be mainly due to the difference of ID and isolation efficiency for τ_h between the data and MC, and thus we did not estimate the acceptance for $Z \to \tau\tau$ correctly.

Table 1: Summary of $Z \to \tau\tau$ event candidates of an isolated electron/muon (ℓ) and a hadronically tau lepton (τ_h) in Run IB [7].

	N_{data}^{OS-LS}	N_{MC}^{Z}	Ratio
e	54±8.1	67.0±3.7	0.81±0.12
μ	22±5.2	29.8±2.5	0.74±0.18

3 Determination of production cross section and upper limit for stop pair

In Section 2, we pointed out the difference in terms of the τ_h ID and isolation efficiency between the data and MC. We need to include the scale factor of τ_h in the acceptance. Then the number of events expected from the MC including the scale factor of τ_h is written as follows:

$$\begin{aligned} N_Z^{MC} &= N_Z^{obs} - N_Z^{BG} \\ &= \left[\sigma_Z \cdot B(Z \to \tau\tau) \cdot \int \mathcal{L}\, dt\right] \times B_{\ell\tau_h} \times A_Z \ , \end{aligned} \tag{7}$$

where, N_Z^{obs}, N_Z^{BG}, and N_Z^{MC} are the number of candidates in the data, expected backgrounds, and expected signals, respectively. σ_Z represents the production cross section of Z, $B(Z \to \tau\tau)$ stands for the branching ratio of $Z \to \tau\tau$, and $\int \mathcal{L}\, dt$ refers to the integrated luminosity. $B_{\ell\tau_h}$ is the branching ratio of di-tau decay in which one of the taus decays into the leptonic channel and the other into the hadronic channel, which is calculated as follows:

$$\begin{aligned} B_{\ell\tau_h} &= 2 \times B(\tau \to \ell\nu\bar{\nu}) \cdot B(\tau \to \tau_h \nu) \\ &\simeq 2 \times 0.36 \times 0.64 = 0.46 \ . \end{aligned} \tag{8}$$

A_Z is the acceptance for $Z \to \tau\tau$ events and written as follows:

$$A_Z = A_Z^{MC} \cdot \epsilon_Z^{trg} \times f_\ell \cdot f_{\tau_h} \ , \tag{9}$$

where A_Z^{MC} is the acceptance for $Z \to \tau\tau$ by calculated by MC, and ϵ_Z^{trg} is the trigger efficiency. f_ℓ and f_{τ_h} are the MC scale factors for the ID and isolation efficiencies of lepton and τ_h respectively. f_ℓ has been already studied in Refs. [12] and [13]. However, f_{τ_h} has not been studied yet due to its difficulty.

Since our final signature of $\tilde{t}_1\bar{\tilde{t}}_1$ is one lepton, one hadronically decaying tau lepton, and two jets, we expect the similar difference between the data and MC will be seen in the stop analysis as well and need to include the scale factor for the τ_h ID and isolation efficiency to the acceptance for $\tilde{t}_1\bar{\tilde{t}}_1$. Assuming f_ℓ and f_{τ_h} for $\tilde{t}_1\bar{\tilde{t}}_1$ are the same values as those for $Z \to \tau\tau$, the number of events expected from MC for $\tilde{t}_1\bar{\tilde{t}}_1$ is written as follows:

$$N_{\tilde{t}_1\bar{\tilde{t}}_1}^{MC} = N_{\tilde{t}_1\bar{\tilde{t}}_1}^{obs} - N_{\tilde{t}_1\bar{\tilde{t}}_1}^{BG}$$

$$
\begin{aligned}
&= \left(\sigma_{\tilde{t}_1\bar{\tilde{t}}_1} \cdot B(\tilde{t}_1 \to \tau^+ b)^2 \cdot \int \mathcal{L}\, dt\right) \times B_{\ell\tau_h} \times A_{\tilde{t}_1\bar{\tilde{t}}_1} \\
&= \left(\sigma_{\tilde{t}_1\bar{\tilde{t}}_1} \cdot B(\tilde{t}_1 \to \tau^+ b)^2 \cdot \int \mathcal{L}\, dt\right) \times B_{\ell\tau_h} \times A^{MC}_{\tilde{t}_1\bar{\tilde{t}}_1} \cdot \epsilon^{trg}_{\tilde{t}_1\bar{\tilde{t}}_1} \times f_\ell \cdot f_{\tau_h} \,, \qquad (10)
\end{aligned}
$$

where, $N^{obs}_{\tilde{t}_1\bar{\tilde{t}}_1}$, $N^{BG}_{\tilde{t}_1\bar{\tilde{t}}_1}$, and $N^{MC}_{\tilde{t}_1\bar{\tilde{t}}_1}$ are the number of candidates from the data, expected backgrounds, and expected signals for $\tilde{t}_1\bar{\tilde{t}}_1$ production, respectively; $\sigma_{\tilde{t}_1\bar{\tilde{t}}_1}$ is the production cross section of $\tilde{t}_1\bar{\tilde{t}}_1$, and $B(\tilde{t}_1 \to \tau^+ b)$ represents the branching ratio of $\tilde{t}_1 \to \tau^+ b$; $A_{\tilde{t}_1\bar{\tilde{t}}_1}$ is the acceptance for $\tilde{t}_1\bar{\tilde{t}}_1 \to \tau^+ b \tau^- \bar{b}$, while $A^{MC}_{\tilde{t}_1\bar{\tilde{t}}_1}$ denotes the acceptance for $\tilde{t}_1\bar{\tilde{t}}_1 \to \tau^+ b \tau^- \bar{b}$ calculated from MC with $\epsilon^{trg}_{\tilde{t}_1\bar{\tilde{t}}_1}$ being the trigger efficiency.

Our goal is to determine the production cross section of $\tilde{t}_1\bar{\tilde{t}}_1$ events. Both Eqs. (7) and (10) include $\int \mathcal{L}\, dt$, $B_{\ell\tau_h}$, f_ℓ, and f_{τ_h} as their common parameters. Therefore by combining the two equations, we can cancel those common parameters and obtain the production cross section of $\tilde{t}_1\bar{\tilde{t}}_1$ as follows:

$$
\begin{aligned}
\sigma_{\tilde{t}_1\bar{\tilde{t}}_1} &= \frac{N^{obs}_{\tilde{t}_1\bar{\tilde{t}}_1} - N^{BG}_{\tilde{t}_1\bar{\tilde{t}}_1}}{A_{\tilde{t}_1\bar{\tilde{t}}_1} B_{\ell\tau_h} \int \mathcal{L}\, dt} \\
&= \frac{N^{obs}_{\tilde{t}_1\bar{\tilde{t}}_1} - N^{BG}_{\tilde{t}_1\bar{\tilde{t}}_1}}{A^{MC}_{\tilde{t}_1\bar{\tilde{t}}_1} \cdot \varepsilon^{trg}_{\tilde{t}_1\bar{\tilde{t}}_1} \cdot \left(\dfrac{N^{obs}_Z - N^{BG}_Z}{\sigma_Z \cdot B(Z \to \tau\tau) \cdot A^{MC}_Z \cdot \varepsilon^{trg}_Z} \right)} \\
&= \left(\frac{N^{obs}_{\tilde{t}_1\bar{\tilde{t}}_1} - N^{BG}_{\tilde{t}_1\bar{\tilde{t}}_1}}{N^{obs}_Z - N^{BG}_Z} \right) \cdot \left(\frac{A^{MC}_Z \cdot \varepsilon^{trg}_Z}{A^{MC}_{\tilde{t}_1\bar{\tilde{t}}_1} \cdot \varepsilon^{trg}_{\tilde{t}_1\bar{\tilde{t}}_1}} \right) \cdot \sigma_Z \cdot B(Z \to \tau\tau) \,. \qquad (11)
\end{aligned}
$$

In the normalization using $Z \to \tau\tau$ events, we have two merits and one demerit. One of the merits is cancellation of several parameters mentioned above. The other merit is reduction of systematic uncertainties of the identification and isolation of lepton and τ_h. The demerit of this method is to involve large uncertainties from the statistical error from the $Z \to \tau\tau$ data. Therefore, we show two studies for our analysis later. One is for $Z \to \tau\tau$ events and the other is for $\tilde{t}_1\bar{\tilde{t}}_1$ events.

4 Baseline $e + \tau_h$ Selection

4.1 Central Electron Selection

This analysis begins with the low p_T electron dataset (ECLB) on Silo BPAD. The integrated luminosity for the dataset is 19.7 pb^{-1} for Run IA and 84.9 pb^{-1} for Run IB. Table 2 shows the Level 2 (L2) and Level (L3) triggers we explicitly require for our analysis. The L2 and L3 trigger efficiencies are given in Refs. [14] and [15] for Run IA and Refs. [16] and [17] for Run IB. The prescaled luminosity for the L2 trigger for Run IB is 73.6 ± 3.0 pb^{-1} [18].

We require at least one well-identified electron in the central region ($|\eta_{det}| < 1$) with $p_T(e) \equiv E^{em}_T \geq 10$ GeV/c, $p^{trk}_T \geq 8$ GeV/c, $|z^{electron}_0 - z_{vtx}| \leq 5$ cm, and $|z_{vtx}| \leq 60$

Table 2: Electron trigger dataset for baseline electron+τ_h selection

Trigger	Run IA	Run IB
Level 2	CEM_9_SEED_9_SH_7_CFT_9_2*	CEM_8_CFT_7_5_XCES*
Level 3	ELE1_CEM_8_6* ELE1_CEM_9*	ELEB_CEM_8_6*

Table 3: Electron identification quality cuts

$E_T^{em} \geq 10$ GeV, $p_T^{trk} \geq 8$ GeV/c, $\lvert\eta_{det}\rvert < 1.0$
$E^{em}/p^{trk} \leq 1.8$
$\chi^2_{strip} \leq 10.0$
$\chi^2_{wire} \leq 10.0$
$\lvert\Delta x\rvert \leq 1.5$ cm, $\lvert\Delta z\rvert \leq 3.0$ cm
$E^{had}/E^{em} \leq 0.05$
$L_{share} \leq 0.2$
Fiducial (`$C_ELE/fidele.cdf`)
Conversion Removal (`$C_TOP/convert2.cdf`)

cm. The electron identification criteria are summarized in Table 3, which are basically the same as the standard electron quality cuts for the top sample [19].

4.2 $Z \to ee$ Removal

Since the second leg electron from $Z \to ee$ can be misidentified as one prong τ_h object, we strictly remove the Z events by using the calorimeter information and the track information (see Table 4).

4.3 Lepton Isolation

After the Z removal, the central lepton is required to be isolated. We apply the same calorimeter and track isolation cuts as those in the SUSY analysis described in Ref. [13]:

$$\begin{aligned} ISO^{cal} &\equiv \sum_{\Delta R<0.4} E_T^{cal,i} - E_T^{clu,\ell} < 4 \text{ GeV} , \\ ISO^{trk} &\equiv \sum_{\Delta R<0.4} p_T^{trk} - p_T^{trk,\ell} < 4 \text{ GeV}/c , \end{aligned}$$

where $E_T^{cal,i} \equiv E_T^{em,i} + E_T^{had,i}$ represents the energy deposit on the ith calorimeter tower, and $E_T^{clu,\ell}$ is the cluster energy deposited on the calorimeter by the lepton ℓ.

Table 4: Cuts for $Z \to ee$ removal.

Calorimeter-based removal	**Track-based removal** ($C_TOP/tauzee.cdf [10])
$E_T^{em} > 8$ GeV	$p_T^{trk} > 10$ GeV$/c$
	$I^{trk}(\Delta R = 0.4) \leq 0.05$
$E^{had}/E^{em} < 0.12$	EM Fraction > 0.7
	$\lvert z_0^{trk} - z_0^{electron} \rvert \leq 8$ cm
Opposite sign charge	Opposite sign charge
76 GeV$/c^2 < M(ee)^{cal} < 106$ GeV$/c^2$	76 GeV$/c^2 < M(ee)^{trk} < 106$ GeV$/c^2$

4.4 Central τ_h Selection

We require the event to have at least one TAUO bank in the central region ($|\eta_{det}| < 1.0$), whose cluster E_T ($\equiv E_T^{clu}$) has a minimum of 4 GeV with

$$p_T(\tau_h) \;\; \equiv p_T^{trk+\pi^0} \equiv \sum_{10^\circ cone} p_T^{trk} + E_T^{em(\pi^0)} \;\; \geq \;\; 15 \text{ GeV}/c \; .$$

The same τ_h identification code in the top dilepton ($\ell + \tau_h$) analysis [10] is applied for the TAUO banks. The τ_h identification quality cuts are summarized in Table 5.

4.5 Baseline Sample

We select events with a central lepton with $p_T(\ell) \geq 10$ GeV$/c$ and a hadronically decaying τ lepton with $p_T(\tau_h) \geq 15$ GeV$/c$ from the Run IB low p_T electron/muon trigger datasets. A total of 479 opposite sign (OS) $e + \tau_h$ events survive the selection, while 251 like sign (LS) $e + \tau_h$ events are retained.

5 Study of Background Processes

5.1 Monte Carlo Samples

Table 6 shows a list of dominant sources of the $e + \tau_h$ events in our baseline sample. In the present analysis, we generated the Monte Carlo (MC) samples listed in Table 7 with the CTEQ4L parton distribution functions (PDFs)[20]. The MC samples of $\gamma^*/Z \to \tau\tau$ are generated by ISAJET[21] with $5 \leq q_T \leq 500$ GeV$/c$ which effectively reproduces the multiplicity and E_T distributions of jets in Z boson production[22]. VECBOS + HERWIG are used for studying the $W, Z+ \geq n$ jets events. We choose $Q^2 = <p_T>^2$ for the QCD parameter of renormalization and fragmentation in VECBOS and HERWIG. We normalize the VECBOS cross section by the r-factor [23]. The VECBOS samples of $W(\to \tau\nu) \geq n$ jets and $Z(\to \tau\tau) \geq n$ jets are generated by replacing electron with τ at the GENP level. TAUOLA[24] and QQ[25] are used to simulate τ and b decays, respectively. We use QFL$'$

Table 5: τ_h identification quality cuts [10]

Number of tracks:	1 or 3 ($\lvert\sum_i Q_i\rvert = 1$) in 10° cone
Number of π^0's:	< 3
E/p:	$0.5 < \dfrac{E_T^{clu}}{p_T^{trk+\pi^0}} < 2.0$ (1-prong)
	$0.5 < \dfrac{E_T^{clu}}{p_T^{trk+\pi^0}} < 1.5$ (3-prong)
Sliding RMS cluster width:	$\sigma_{cl} < 0.11 - 0.025 \times E_T^{clu}/100$ (1-prong)
	$\sigma_{cl} < 0.13 - 0.034 \times E_T^{clu}/100$ (3-prong)
Mass:	$M(\tau_h) \equiv M(trk, \pi^0) < 1.8$ GeV$/c^2$
Isolation:	$I^{trk} < 1$ GeV$/c$
Electron removal:	Reject
	(a) 1-prong with $E_T^{clu}/p_T^{trk} < 4$, EM fraction > 0.9 or
	(b) clusters with EM fraction > 0.95
Muon removal:	Reject cluster with
	(a) $E_T^{clu} < 8$ GeV, $0.05 < E^{em} < 2$ GeV, $0.5 < E^{had} < 5$ GeV or
	(b) a muon stub with $\lvert\phi_\tau - \phi_{stub}\rvert < 15^\circ$ as muon

Table 6: Sources to $\ell + \tau_h$ events

real ℓ + real τ_h	real ℓ + fake τ_h	real τ_h + fake ℓ	fake ℓ + fake τ_h
$\gamma^*/Z \to \tau\tau$	$W(\to \ell\nu)$ + jets	$W(\to \tau\nu)$ + jets	
	$W(\to \tau\nu \to \ell\nu\nu\nu)$ + jets		
$t\bar{t}$	$t\bar{t}$	$t\bar{t}$	
diboson	diboson	diboson	
QCD($b\bar{b}/c\bar{c}$)	QCD($b\bar{b}/c\bar{c}$)	QCD($b\bar{b}/c\bar{c}$)	QCD
	$\gamma^*/Z \to \ell\ell$		

Table 7: Summary of Monte Carlo samples

Process	Monte Carlo	$\sigma \cdot B$
$Z \to \tau\tau$	ISAJET	231±12 pb [26]
$\gamma^* \to \tau\tau$	ISAJET	259±57 pb [27]
$Z(\to \tau\tau)$ + jets	VECBOS + HERWIG	$\sigma_{\text{VECBOS}} \times r$-factor
$W(\to e\nu)$ + jets	VECBOS + HERWIG	$\sigma_{\text{VECBOS}} \times r$-factor
$W(\to \tau\nu)$ + jets	VECBOS + HERWIG	$\sigma_{\text{VECBOS}} \times r$-factor
$t\bar{t}$	ISAJET	$6.5\pm^{1.7}_{1.4}$ pb [28]
WW	ISAJET	$10.2\pm^{6.3}_{5.1} \pm 1.6$ pb [29]
WZ	ISAJET	2.66 pb [30]
ZZ	ISAJET	1.08 pb [31]

for the detector simulation. The MC study of QCD events are not carried out in the present analysis. However, most of the QCD events in the OS $\ell+\tau_h$ sample are estimated by using the LS $\ell + \tau_h$ sample (see Section 5.2).

We calculate the expected yield as follows:

$$\begin{aligned} N &= [\sigma \cdot B \times \textstyle\int \mathcal{L}\, dt] \times \frac{\#\text{ of events passed}}{\#\text{ of events generated}} \\ &\quad \times [\text{L1 \& L2 \& L3 trigger efficiencies}] \\ &\quad \times [\text{MC scale factor for lepton ID cut}] \\ &\quad \times [\text{MC scale factor for lepton isolation cut}]. \end{aligned}$$

The product of the production cross section and the branching ratio ($\sigma \cdot B$) is taken from the CDF measurements [26, 27, 28, 29] and the NLO calculations [30, 31]. We assume $\sigma \cdot B(Z \to ee) = \sigma \cdot B(Z \to \mu\mu) = \sigma \cdot B(Z \to \tau\tau)$.

The scale factors for the electron isolation and ID cut efficiencies in the MC samples are obtained to be 98% [13] and 97% [12], respectively.

5.2 QCD Background

There are two major background sources of the LS events: (i) QCD jets (gluons, light quarks, $b\bar{b}/c\bar{c}$) and (ii) $W(\rightarrow \ell\nu)$ + jets. Of them, the QCD background is the most difficult one to estimate with MC because of the large cross section and the low fake rate. Both ℓ and τ_h from the QCD events are dominantly due to the fake. Since there is no or weak charge correlation between ℓ and τ_h, we expect to have both OS and LS events at an equal rate. Therefore, we calculate the expected number of OS events as follows:

$$\text{Expected number of OS events} = \text{MC(OS} - \text{LS)} + \text{LS Data.} \tag{12}$$

It should be noted that there is a small charge correlation between lepton and τ_h for W + jets. The ratio of OS to LS events for W + jets is expected to be 4~3 to 1 from VECBOS + HERWIG. Almost all the events for $\tilde{t}_1\bar{\tilde{t}}_1$, $Z \rightarrow \tau\tau$, $t\bar{t}$, and diboson production are OS events, namely the ratio of OS to LS events is 1 to 0.

5.3 Comparison with Monte Carlo Events after baseline selection

Table 8 shows a summary of yields in the data and MC events. The expected number of OS events is estimated to be 447.3±16.3 using the method mentioned in the previous subsection, while the number of OS events in the data is 479±22(stat). Figure 1 shows the distributions of transverse energy of electron ($E_T(e)$), transverse momentum of τ_h ($p_T(\tau_h)$), azimuthal angle between electron and τ_h ($\Delta\phi(e, \tau_h)$), azimuthal angle between electron and $\vec{\not{E}}_T$ ($\Delta\phi(e, \vec{\not{E}}_T)$), missing E_T ($\not{E}_T$), and invariant mass between electron and τ_h ($M(e, \tau_h)$), for the data and expected OS events, respectively. $\not{E}_T$ is only corrected for muons with $p_T \geq 10$ GeV/c. The difference between OS data and MC(OS−LS)+LS data can be seen in the low-value regions of $E_T(e)$, $p_T(\tau_h)$, $\not{E}_T$, and $M(e, \tau_h)$. We expect these differences are caused by the slight charge correlations of the QCD events.

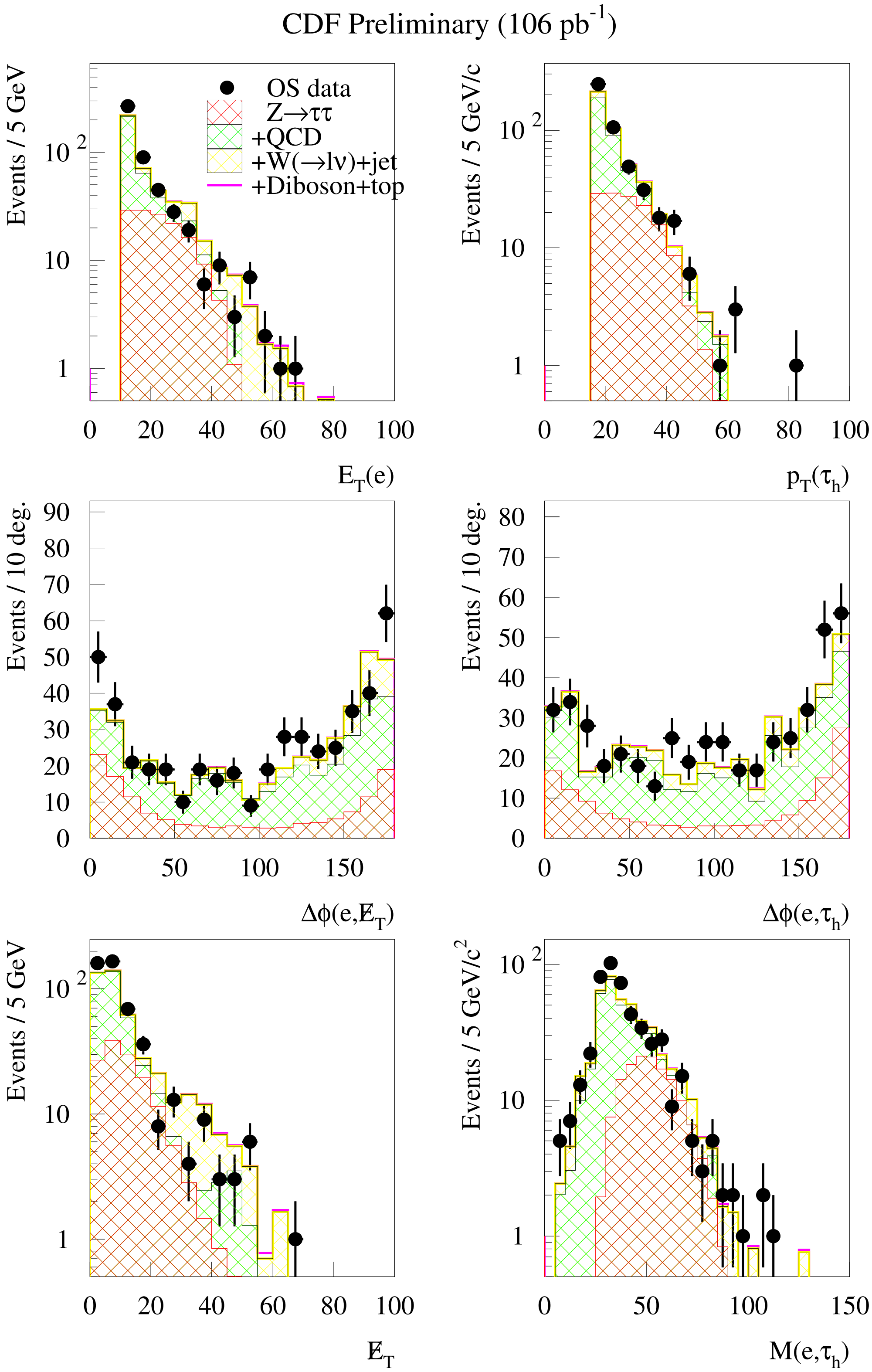

Figure 1: Distributions of $E_T(e)$, $p_T(\tau_h)$, $\Delta\phi(e,\tau_h)$, $\Delta\phi(e,\not{E}_T)$, $\not{E}_T$ $M(e,\tau_h)$, for data and expectation of OS events after the baseline selection.

Table 8: Summary of yields of $e + \tau_h$ pairs in the data and MC events after baseline selection. The uncertainty is only statistical.

Low-E_T($\geq$10 GeV) Electron Analysis			
Process	OS	LS	OS−LS
$Z(\to \tau\tau)$	138.5	0.7	137.8±0.8
$\gamma^*(\to \tau\tau)$	2.3	0.0	2.3±0.4
$W(\to e\nu)$	65.3	19.7	45.6±3.6
$W(\to \tau\nu)$	11.3	2.6	8.7±1.3
$t\bar{t}$	0.73	0.10	0.63±0.10
WW	1.01	0.16	0.85±0.07
WZ	0.20	0.10	0.10±0.01
ZZ	0.34	0.08	0.26±0.04
Total background	219.7	23.4	196.3 ± 3.9
Data (IA+IB)	479	251	228±27

6 Event Selection of $Z \to \tau\tau$ events

In Section 5, the sources to the $\ell + \tau_h$ events in our baseline sample are $Z \to \tau\tau$, W+jets, and QCD events. We apply the same cuts as those in CDF note 5251 to our baseline samples in order to obtain the $Z \to \tau\tau$ events with high purity. We first remove the W+jets events from both OS and LS samples by using a cut on the transverse mass between electron and $\not\!\!E_T$: $M_T(e, \not\!\!E_T)$, which is insensitive to the charge correlation. The Figure 2 shows the distributions of $M_T(e, \not\!\!E_T)$ for the data and MC along with the distribution of significance as a function of $M_T(e, \not\!\!E_T)$. Significance is defined as the ratio to expected number of signal to square of expected number of background, where both numbers are obtained from the MC samples. In this case, we use signal for $Z \to \tau\tau$ and background for $W(\to e\nu)$ + jets, respectively. We require

$$M_T(e, \not\!\!E_T) \leq 25 \text{ GeV}/c^2. \tag{13}$$

After applying the $M_T(e, \not\!\!E_T)$ cut, the QCD events become dominant among the LS events. Then, we apply a cut on the transverse momentum of the electron + $\not\!\!E_T$ system: $p_T(e, \not\!\!E_T) \equiv |\vec{E}_T(e) + \vec{\not\!\!E}_T|$. Figure 3 shows the distributions of $p_T(e, \not\!\!E_T)$ for the data and MC after the $M_T(e, \not\!\!E_T)$ cut along with the distribution of significance as a function of $p_T(e, \not\!\!E_T)$, where expected number from QCD is obtained from the LS events in the data.

We require

$$p_T(e, \not\!\!E_T) \geq 25 \text{ GeV}/c^2. \tag{14}$$

These cut values are determined to maximize the significance of $Z \to \tau\tau$ events over each background source. More detailed descriptions can be found in Ref. [7]. As a result of the above cuts, we obtain 69 OS and 8 LS events in the data. The acceptance and trigger efficiency for $Z \to \tau\tau \to e + \tau_h + X$ (A^Z_{MC} and ε^Z_{trg}) are found to be 1.48 ± 0.02 (stat) % and 74.5 %, respectively.

It is possible that the same events are included in both stop and $Z \to \tau\tau$ candidates. Therefore, we separate stop and $Z \to \tau\tau$ events by using the number of jets since the majority of the stop events is expected to have more than two jets as discussed later. We thus apply the jet-veto, namely only 0-jet events are selected after the above two cuts. The jet is defined as $E_T^{raw} > 10$ GeV, $E_T^{corr} > 15$ GeV, and $|\eta_{det}| < 2.4$ with the cone size of $R = 0.4$. It should be noted that JTC96X (EYDD option) is used to calculate the E_T^{corr} of jet. We determine the acceptance of $Z \to \tau\tau$ events with 0-jet by using the measurement of $Z(\to ee) + \geq n$ jets at CDF[32]. We calculate the expected number of $Z \to \tau\tau$ events with 0-jet by multiplying the ratio of 0-jet events to the total (R(0-jet)) obtained from the analysis of $Z(\to ee) + \geq n$ jets as follows:

$$\begin{aligned} R(\text{0-jet}) &= R(\geq 0 \text{ jet}) - R(\geq 1 \text{ jet}) \\ &= 1 - \frac{\sigma_Z(\geq 1 \text{ jet})}{\sigma_Z(\geq 0 \text{ jet})} \\ &= 0.8040 \pm 0.0065(\text{stat+sys}) \pm 0.0238(\text{Jet Def.})\,. \end{aligned} \tag{15}$$

Therefore, the expected number of $Z \to \tau\tau$ events with 0 jet is calculated as follows:

$$N^Z_{expected} = A^Z_{MC} \cdot f_\ell \cdot \varepsilon^Z_{trg} \cdot B_{e\tau_h} \cdot \sigma \cdot B(Z \to \tau\tau) \cdot \int \mathcal{L}\, dt \times R(\text{0-jet})$$

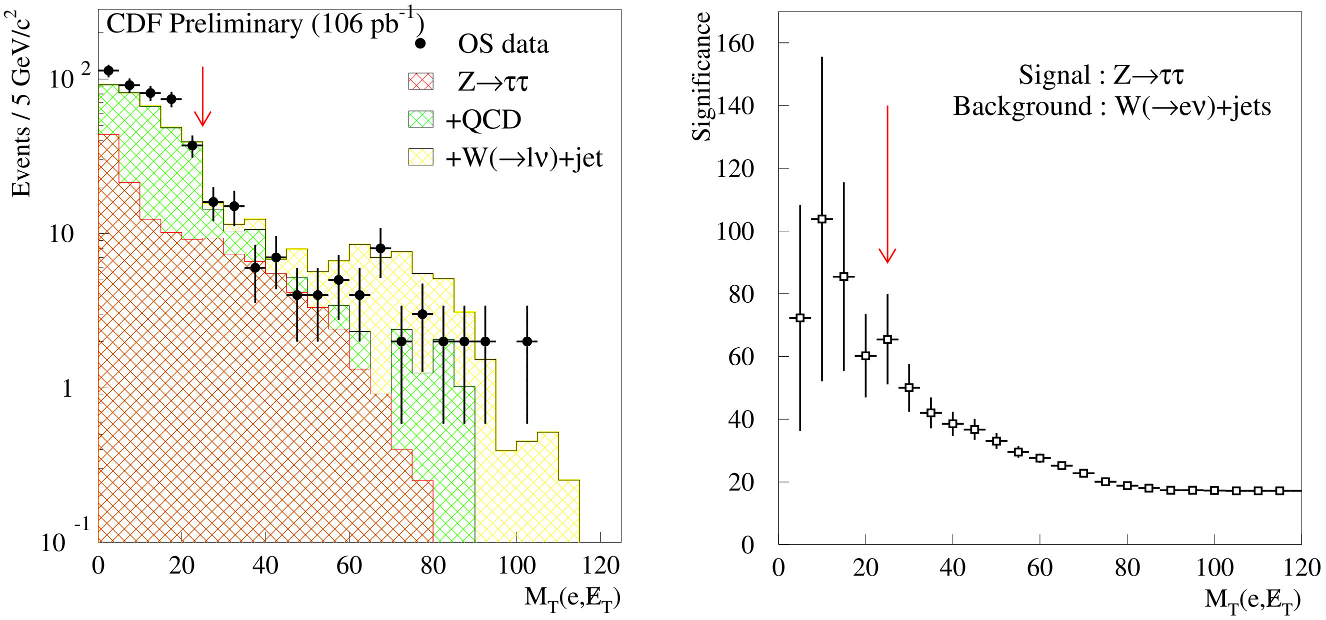

Figure 2: Distributions of $M_T(e, \not{E}_T)$ (left) and significance (right)

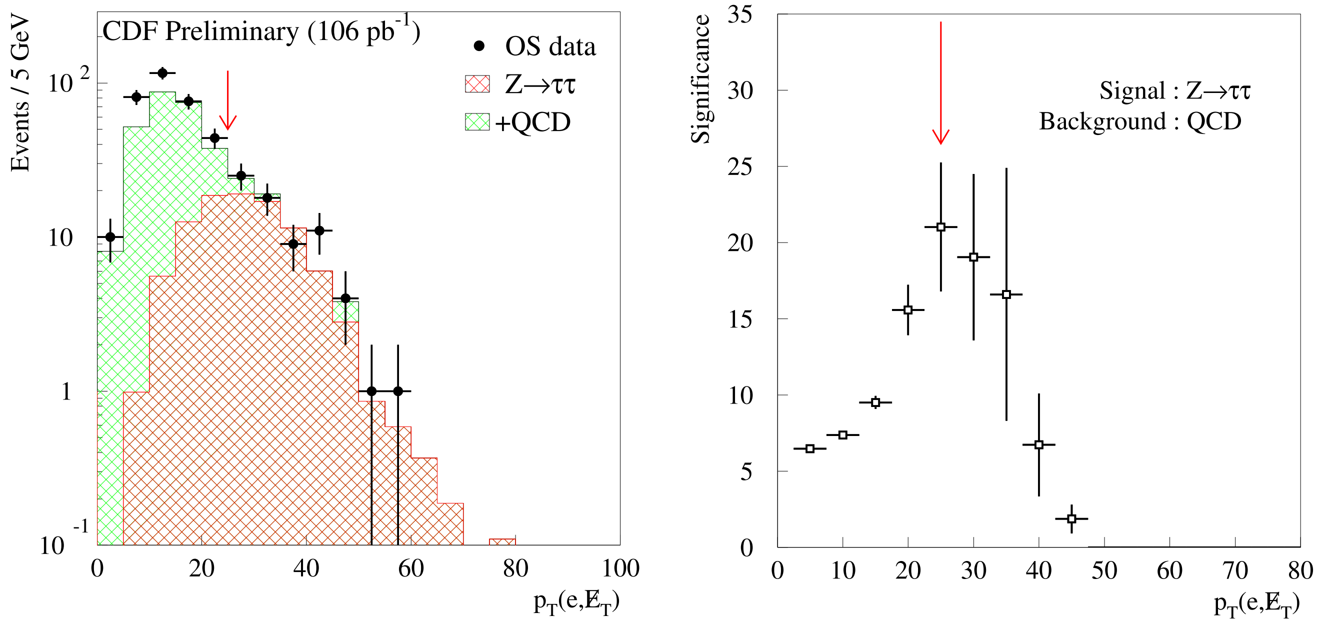

Figure 3: Distributions of $p_T(e, \not{E}_T)$ (left) and significance (right)

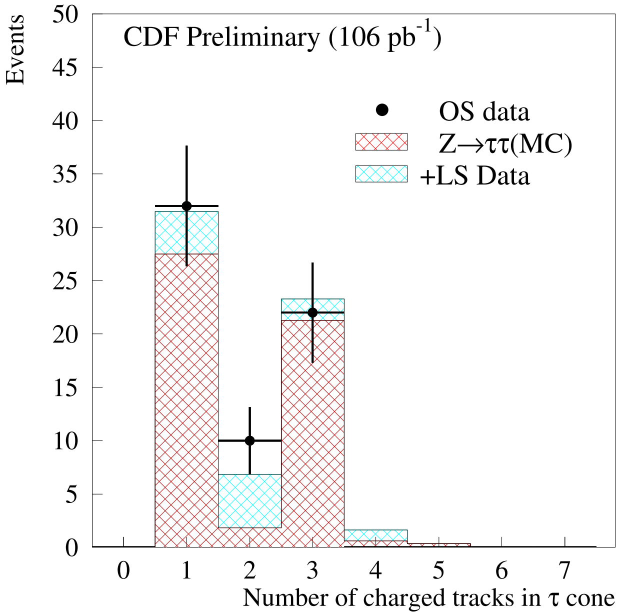

Figure 4: Number of charged tracks in τ cone after $Z(\to \tau\tau) + 0$ jet selection

$$= \quad 47.5 \pm 0.6(\text{stat}) \tag{16}$$

Table 9 shows the number of events in the data and MC for $Z \to \tau\tau$ and W + jets for each cut. Table 10 shows the number of events in the data and MC for $Z \to \tau\tau$ and W + jets after the 0-jet selection. The expected number of $Z \to \tau\tau$ events is $47.2 \pm 0.6(\text{stat}) \pm 2.8(\text{sys})$ from MC. The number of OS events subtracted with background is $45.6 \pm 7.8(\text{stat}) \pm 0.2(\text{sys})$. Figure 4 shows the number of charged tracks in τ cone after $Z(\to \tau\tau) + 0$ jet selection. The selection for 2-prong and $\geq$ 4-prong event is same selection as 1-prong and 3-prong events, respectively. The τ_h charge for 2-prong and $\geq$4-prong events is defined to be the charge of the hightest-p_T track. Figure 5 shows the distributions of OS data and expected background from MC and LS data. We can see one and three tracks excess in the OS data. We obtain the good agreement between MC and data after the 0-jet selection.

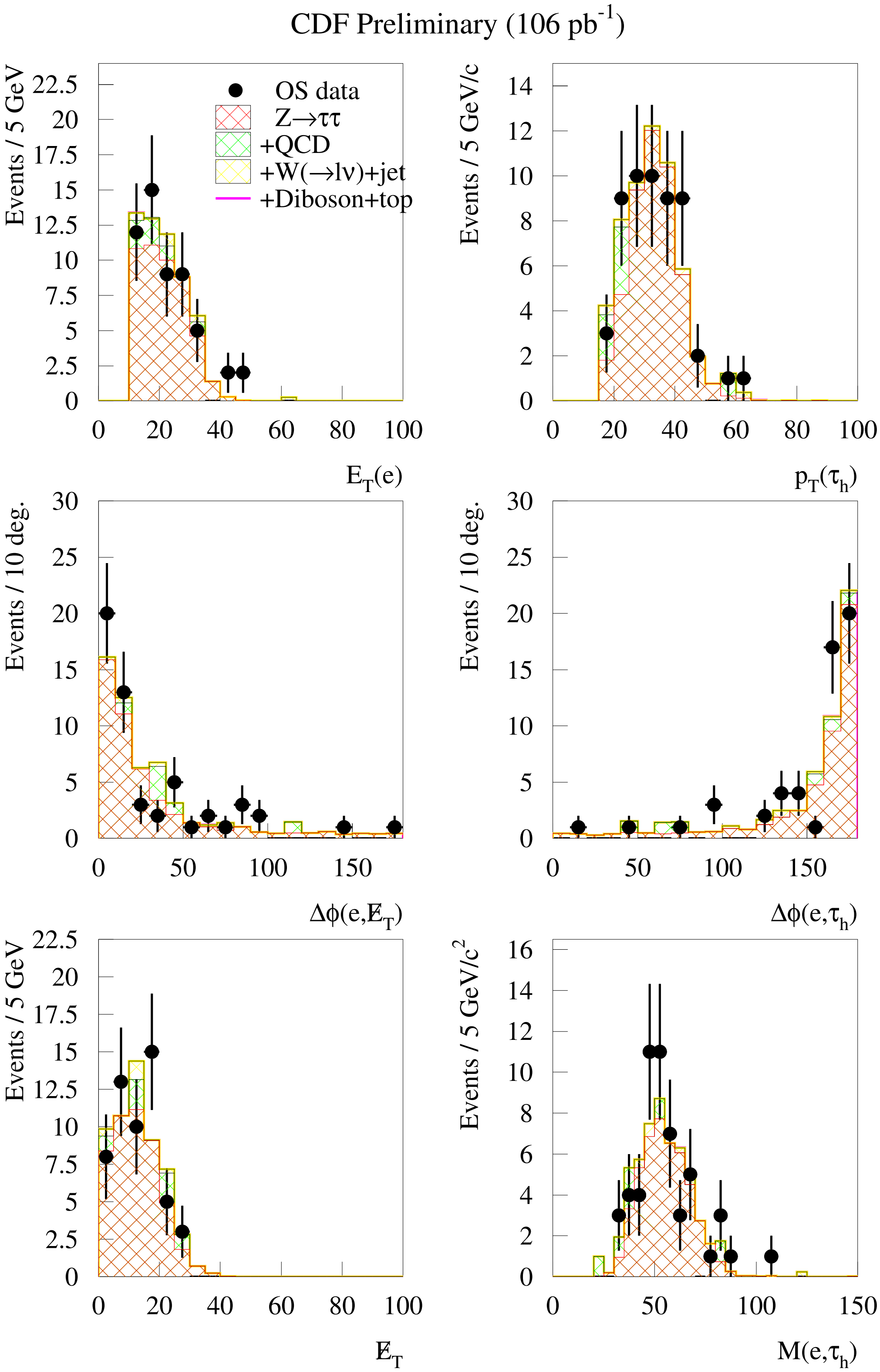

Figure 5: Distributions of $E_T(e)$, $p_T(\tau_h)$, $\Delta\phi(e,\tau_h)$, $\Delta\phi(e,\not{E}_T)$, $\not{E}_T$ and $M(e,\tau_h)$ for data and expectation of OS events after $Z \to \tau\tau$ with 0-jet selection cuts.

Table 9: Number of events in data and MC samples after each cut

[$e + \tau_h$]	$Z(\to \tau\tau)$		$W(\to e\nu)$+jets		Data	
Cut	OS	LS	OS	LS	OS	LS
Baseline	138.5	0.7	65.3	19.7	479	251
$M_T(e, \not{E}_T)$ cut	96.7	0.5	2.2	0.8	396	230
$p_T(e, \not{E}_T)$ cut	59.0	0.4	1.0	0.3	69	8
jet-veto cut	47.5	0.3	0.8	0.3	54	6

Table 10: Summary of yields of $e + \tau_h$ pairs in the data and MC events after $Z \to \tau\tau$ with 0-jet selection cut.

Process	OS	LS
Data	54	6
$Z \to \tau\tau$	$47.5 \pm 0.6 \pm 2.8$	$0.3 \pm 0.1 \pm 0.1$
$\gamma \to \tau\tau$	$0.4 \pm 0.2 \pm 0.1$	$0.0 \pm 0.0 \pm 0.0$
$W(\to \ell\nu, \tau\nu)$+jets	$2.3 \pm 0.6 \pm 0.1$	$0.3 \pm 0.1 \pm 0.1$
Diboson,Top	$0.02 \pm 0.01 \pm 0.01$	$0.00 \pm 0.00 \pm 0.00$
QCD	5.4 ± 2.5	5.4 ± 2.5
Total OS expectation	55.6 ± 2.6(stat) ± 2.8(sys)	

7 Event Selection of $\tilde{t}_1\bar{\tilde{t}}_1$ events

We use ISAJET v7.44 to generate $\tilde{t}_1\bar{\tilde{t}}_1$ events with the CTEQ4L PDFs for our analysis.

We begin with removing the W + jets events from both OS and LS samples by applying the cut on the transverse mass between electron and $\not\!\!E_T$: $M_T(e, \not\!\!E_T)$, which is the same manner as we use for the $Z \to \tau\tau$ selection described in Section 6. In this case, we require

$$M_T(e, \not\!\!E_T) \leq 35 \text{ GeV}/c^2\,. \tag{17}$$

Figure 6 shows the distributions of $M_T(e, \not\!\!E_T)$ for the data and MC events along with the distribution of significance as a function of $M_T(e, \not\!\!E_T)$ in case of the $\tilde{t}_1$ mass being 100 GeV/c^2. For the next step, we apply a cut on the scaler sum of the transverse energy of electron, transverse momentum of τ_h, and $\not\!\!E_T$: $H_T(e, \tau_h, \not\!\!E_T) = E_T(e) + p_T(\tau_h) + \not\!\!E_T$ in order to remove the QCD events which are dominant after the $M_T(e, \not\!\!E_T)$ cut. Figure 7 shows the distributions of $H_T(e, \tau_h, \not\!\!E_T)$ for the data and MC along with the distribution of significance as a function of $H_T(e, \tau_h, \not\!\!E_T)$. We require

$$H_T(e, \tau_h, \not\!\!E_T) \geq 75 \text{ GeV}/c^2\,. \tag{18}$$

It should be noted that the ℓ+τ_h events dominantly result from $Z \to \tau\tau$ after the two cuts described above. Figure 8 shows the distributions of the OS data and the background estimated with the MC and LS data.

Finally, we apply a cut on the number of jets (N_{jet}). The definition of jet here is the same as that for the $Z \to \tau\tau$ analysis in Section 6. Figure 9 shows the distributions of N_{jet} for the data and MC along with the distribution of significance as a function of N_{jet}. We compare the $\tilde{t}_1\bar{\tilde{t}}_1$ events with the $Z \to \tau\tau$ events generated by ISAJET. We require

$$N_{jet} \geq 2\,. \tag{19}$$

Table 11 shows the event selection and trigger efficiencies for $\tilde{t}_1\bar{\tilde{t}}_1 \to \tau^+ b\tau^- \bar{b} \to e\tau_h b\bar{b} + X$ events from 70 to 130 GeV/c^2 for each cut. Figure 10 shows the plot for the cumulative cut efficiency for $\tilde{t}_1\bar{\tilde{t}}_1$ events.

Table 12 shows the number of events in the data and MC for $Z \to \tau\tau$ and $W(\to e\nu)$ + jets for each cut. Table 13 shows the number of events in the data and MC for $Z \to \tau\tau$ and W + jets after the 0-jet selection. No event is obtained after the stop selection, while the number of expected backgrounds is 1.97 $^{+1.01}_{-0.11}$ (stat) $\pm$ 0.15 (sys). The dominant source of the expected background results from $Z \to \tau\tau$ events. In Table 13, the expected number of $Z(\to \tau\tau)$ and $W(\to e\nu$ or $\tau\nu)$ + jets events is calculated with use of VECBOS and HERWIG. For verification, we recalculate the $Z \to \tau\tau$ events using ISAJET. The number of OS, LS, and OS$-$LS events in the $Z \to \tau\tau$ samples are estimated to be 1.64 $\pm$ 0.10 (stat), 0.05 $\pm$ 0.03 (stat), and 1.59 $\pm$ 0.10 (stat), respectively. The estimate of $Z \to \tau\tau$ using VECBOS + HERWIG is consistent with that using ISAJET.

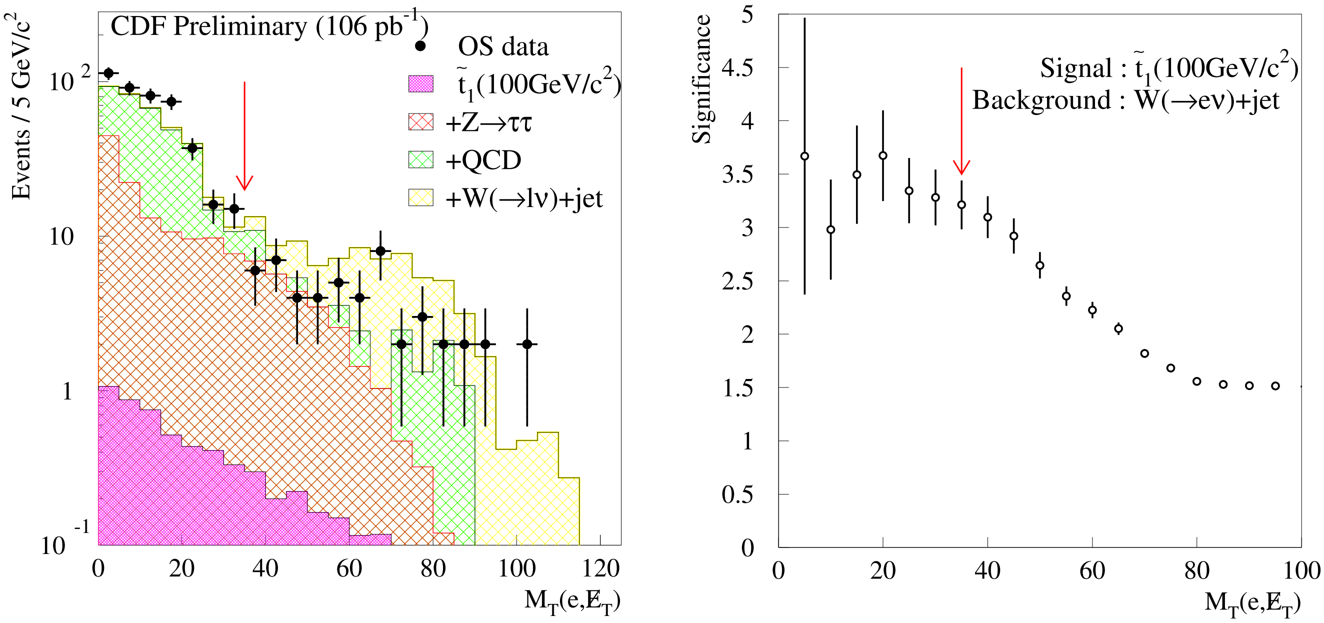

Figure 6: Distributions of $M_T(e, \not{E}_T)$ (left), and significance (right)

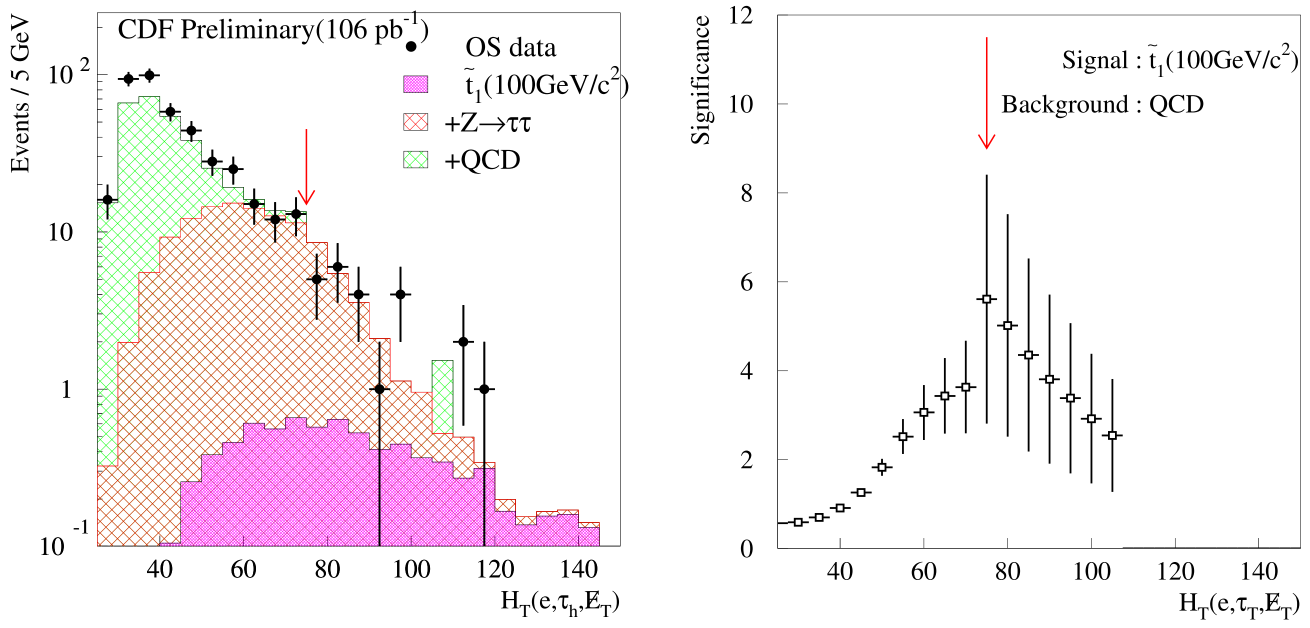

Figure 7: Distributions of $H_T(e, \not{E}_T)$ (left) and significance (right)

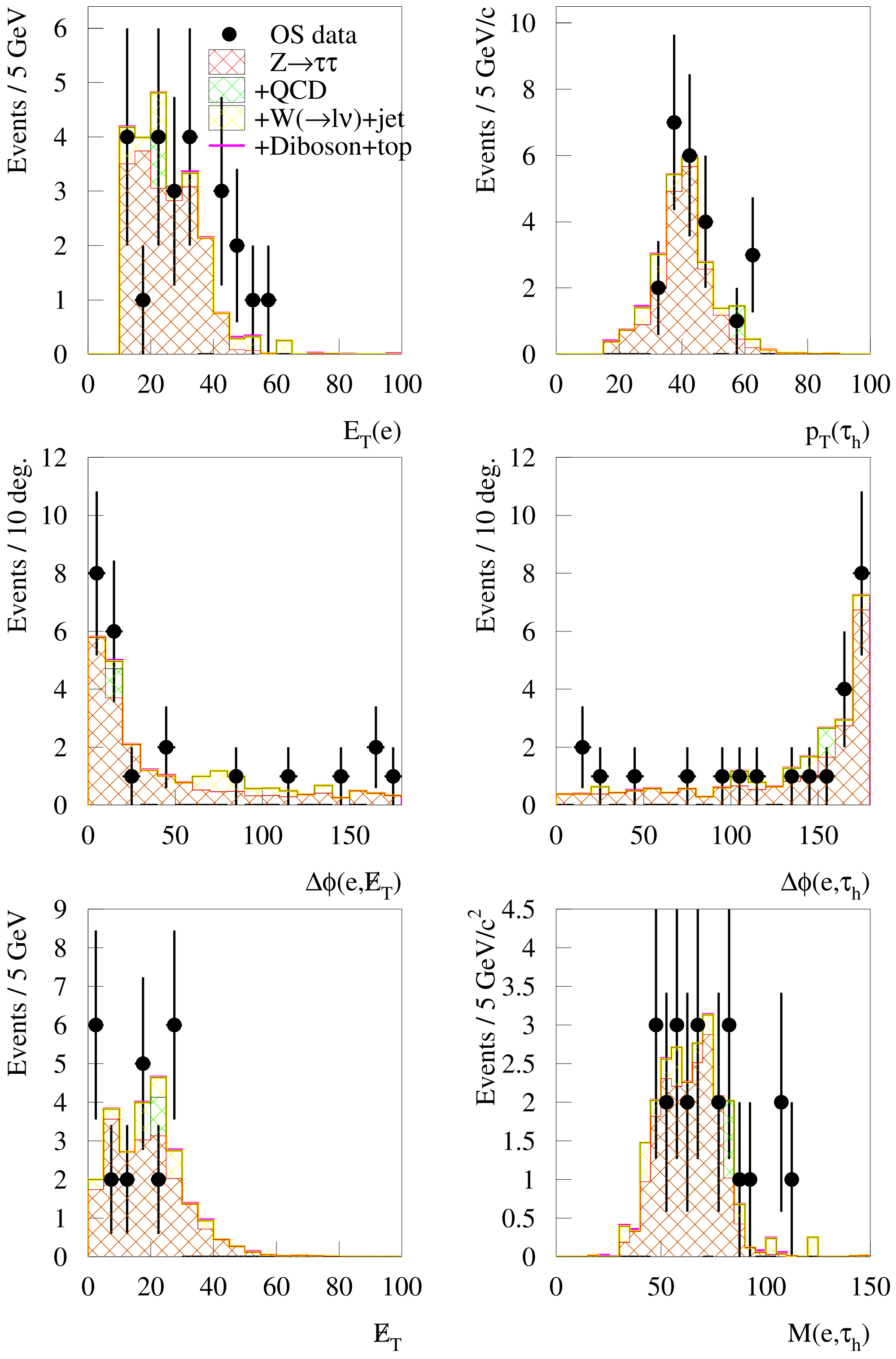

Figure 8: Distributions of $E_T(e)$, $p_T(\tau_h)$, $\Delta\phi(e,\tau_h)$, $\Delta\phi(e,\not{E}_T)$, $\not{E}_T$ $M(e,\tau_h)$, for data and expectation of OS events after $\tilde{t}_1\bar{\tilde{t}}_1$ selection cuts before jet requirement.

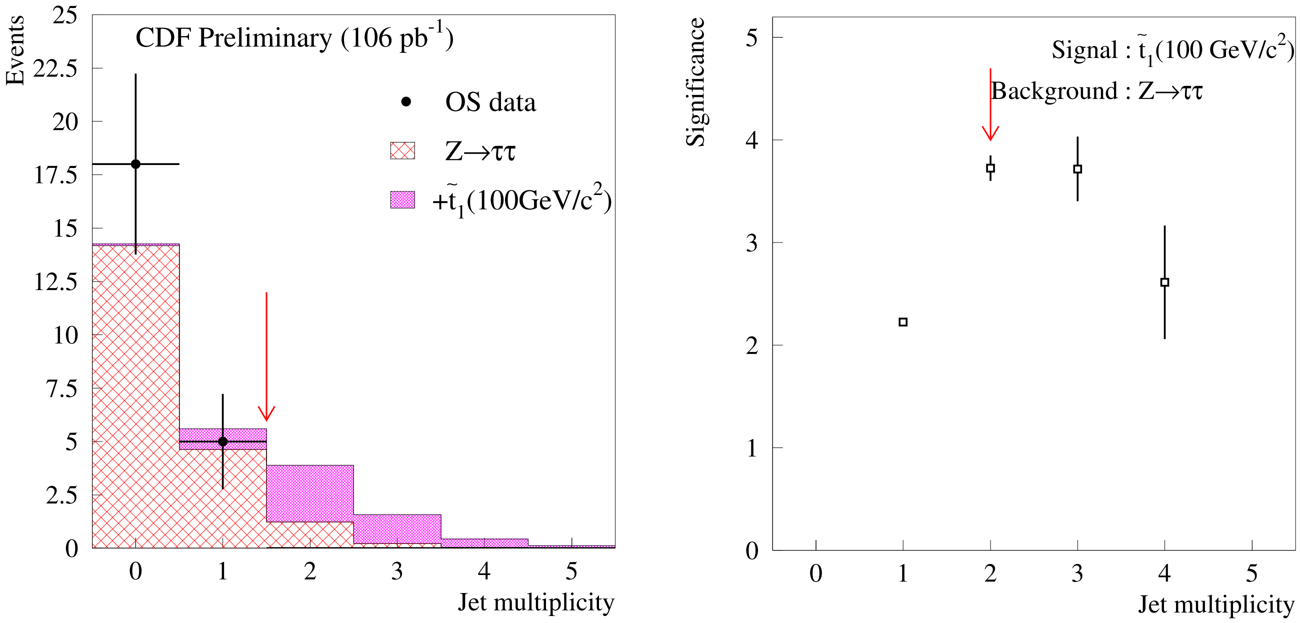

Figure 9: Distributions of the number of jets (left) and significance (right)

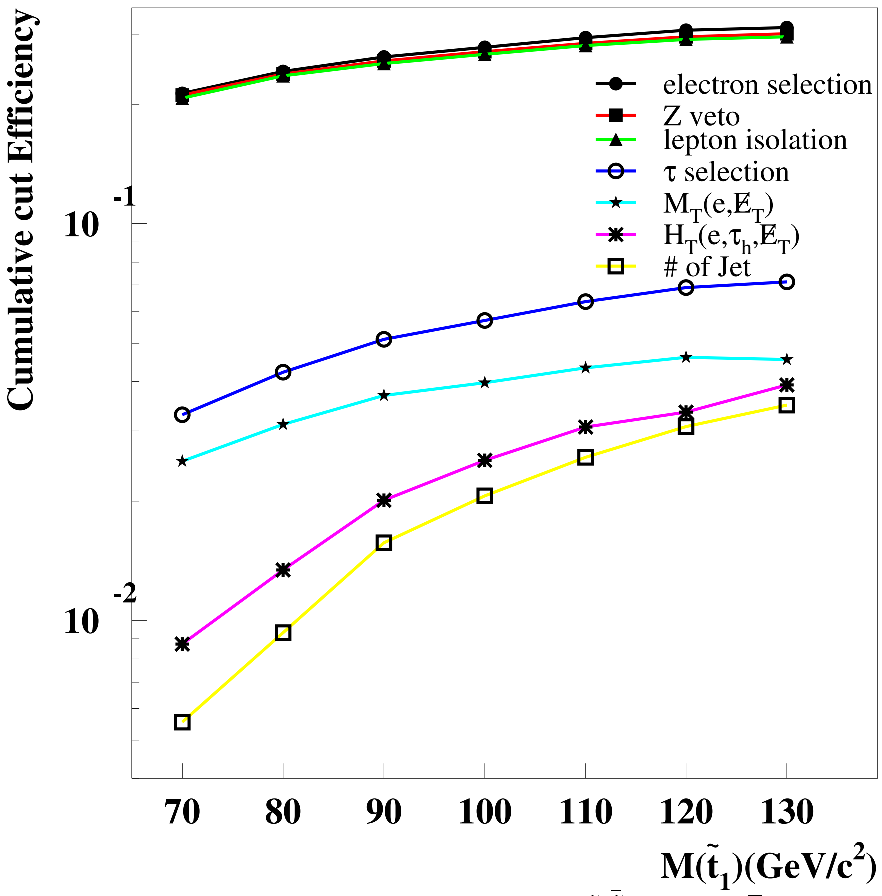

Figure 10: Cumulative cut efficiency for $\tilde{t}_1\bar{\tilde{t}}_1 \to \tau^+ b\tau\bar{b} \to (\ell\nu\nu b)(\tau_h\nu\bar{b})$

Table 11: Event selection and trigger efficiencies (%) for $\tilde{t}_1\bar{\tilde{t}}_1 \to \tau^+ b \tau^- \bar{b} \to e\tau_h b\bar{b} + X$ events from 70 to 130 GeV/c^2 with each cuts.

Cut efficiency (%)							
$M(\tilde{t}_1)$ (GeV/c^2)	70	80	90	100	110	120	130
e selection	21.3	24.2	26.3	27.8	29.4	30.7	31.2
Z veto	98.9	98.3	97.8	97.4	96.9	96.6	95.8
Isolation	98.2	98.3	98.1	98.4	98.4	98.2	98.4
τ_h selection	15.7	17.9	20.0	21.2	22.5	23.5	23.9
$M_T(e, \not{E}_T)$	77.3	74.6	72.9	70.2	68.7	67.1	64.3
$H_T(e, \tau_h, \not{E}_T)$	34.6	43.0	54.5	63.7	70.9	77.3	86.2
N_{jet}	63.6	69.5	78.0	81.3	84.0	86.5	88.9
Total	0.554	0.932	1.57	2.06	2.58	3.08	3.49
Trigger efficiency	77.1	77.5	77.6	78.1	78.1	78.5	78.5

Table 12: Number of events in data and MC samples after each cut

[$e + \tau_h$]	$Z(\to \tau\tau)$		$W(\to e\nu)$+jets		Data	
Cut	OS	LS	OS	LS	OS	LS
Baseline	138.5	0.7	65.3	19.7	479	251
$M_T(e, \not{E}_T)$ cut	113.4	0.6	6.0	2.0	427	238
$H_T(e, \tau_h, \not{E}_T)$ cut	19.3	0.1	2.3	0.7	23	1
N_{jet}	1.66	0.00	0.12	0.03	0	0

Table 13: Summary of yields of $e + \tau_h$ pairs in the data and MC events after $\tilde{t}_1\bar{\tilde{t}}_1$ selection cut.

Process	OS	LS
Data	0	0
$Z \to \tau\tau$	1.66 ± 0.09(stat) ± 0.14(sys)	0.00 ± 0.00 ± 0.00
$\gamma \to \tau\tau$	0.01 ± 0.01 ± 0.01	0.00 ± 0.00 ± 0.00
$W(\to e\nu)$+jets	0.12 ± 0.04 ± 0.01	0.03 ± 0.01 ± 0.01
$W(\to \tau\nu)$+jets	0.02 ± 0.02 ± 0.01	0.00 ± 0.00 ± 0.00
Diboson	0.06 ± 0.01 ± 0.02	0.01 ± 0.01 ± 0.01
Top	0.10 ± 0.03 ± 0.03	0.00 ± 0.00 ± 0.00
QCD	$0\,^{+1}_{-0}$	$0\,^{+1}_{-0}$
Total OS expectation	$1.97\,^{+1.01}_{-0.11}\,\pm 0.15$	

8 Systematic Uncertainties

We experimentally measure the production cross section ($\sigma_{\tilde{t}_1\bar{\tilde{t}}_1}$) and the branching ratio ($\mathrm{B}(\tilde{t}_1 \to \tau^+ b)$) as follows:

$$
\begin{aligned}
\sigma_{\tilde{t}_1\bar{\tilde{t}}_1} \cdot B(\tilde{t}_1 \to \tau^+ b)^2 &= \frac{N^{95\%C.L.}_{\tilde{t}_1\bar{\tilde{t}}_1}}{A_{\tilde{t}_1\bar{\tilde{t}}_1} B_{\ell\tau_h} \int \mathcal{L}\, dt} \\
&= \left(\frac{N^{95\%C.L.}_{\tilde{t}_1\bar{\tilde{t}}_1}}{N^{obs}_Z - N^{BG}_Z} \right) \left(\frac{A^{MC}_Z \cdot \varepsilon^{trg}_Z}{A^{MC}_{\tilde{t}_1\bar{\tilde{t}}_1} \cdot \varepsilon^{trg}_{\tilde{t}_1\bar{\tilde{t}}_1}} \right) \cdot \sigma_Z \cdot B(Z \to \tau\tau) \cdot R(0\text{-jet})
\end{aligned}
\tag{20}
$$

The evaluation of systematic uncertainties due to $Z \to \tau\tau$ and $\tilde{t}_1\bar{\tilde{t}}_1$ events is described below.

8.1 Cancellation and Reduced Term of Systematic Uncertainties

8.1.1 Cancellation Term of Systematic Uncertainties

We calculate the cross section of $\tilde{t}_1\bar{\tilde{t}}_1$ events normalized by $Z \to \tau\tau$ events. By normalizing by $Z \to \tau\tau$ events, some systematic uncertainties are canceled. They are the luminosity, the z-vertex efficiency, and the τ branching ratio. It should be noted that the uncertainty arising from the luminosity measurement is included in the Z production cross section measurement at CDF. The reduced source of systematic uncertainties are identification and isolation from lepton and τ_h.

8.1.2 Systematic Uncertainty of Trigger Efficiency

The systematic uncertainty of the trigger efficiency is assigned as the maximum difference between the ratio of trigger efficiency of $Z \to \tau\tau$ to that of $\tilde{t}_1\bar{\tilde{t}}_1$ event by varying the parameterized curves by one standard deviation for the L1, L2 and L3 triggers.

8.2 Systematic Uncertainties of $Z(\to \tau\tau)$ Events

8.2.1 Cross Section of $Z(\to \tau\tau)+ \geq n$ Jets Events

We use the cross section of $Z(\to ee)+ \geq n$ jets as that of $Z(\to \tau\tau)+ \geq n$ jets, assuming the lepton universality. Therefore we employ the uncertainty caused by the error of the cross section of $Z(\to ee)+ \geq n$ jets [35]. Furthermore, we employ the uncertainty caused by the error from the ratio of $Z(\to ee)+ \geq n$ jets cross section [32].

8.2.2 Parton Distribution

The choice of the PDFs affects the total cross section, the relative contributions of the gg and $q\bar{q}$ subprocesses, and the event kinematics. Our standard choice of the PDFs used in all MC simulations is CTEQ4L [20]. The systematic uncertainty due to the different PDFs is estimated by comparing the acceptance of $Z \to \tau\tau$ events with that for other PDFs. Here we use MRS(G) [33] and GRV94LO [34] for the comparison.

8.3 Systematic Uncertainties for $\tilde{t}_1\bar{\tilde{t}}_1$ Events

8.3.1 Gluon Radiation

We use `$ISAJET_LIBRARY/source/decjet.f` for excluding jet generated by final gluon radiation (FSR) via the parton shower fragmentation. We determine the effect on the acceptance due to gluon radiation on the acceptance by taking the difference between the acceptance with FSR "on" and that with FSR "off". Furthermore, assuming the size of the effect for initial state gluon radiation (ISR) is the same as FSR effect, the total magnitude of ISR and FRS effect is calculated by adding the ISR and FSR effects quadrature.

8.3.2 Q^2 Dependence

The nominal Q_0^2 in the two body process in ISAJET is defined as

$$Q_0^2 = \max\left(\frac{2\hat{s}\hat{t}\hat{u}}{\hat{s}^2+\hat{t}^2+\hat{u}^2}, 4M_{\tilde{t}}^2\right)$$

We calculate the nominal acceptance with two choices of 4 Q_0^2 and 0.25 Q_0^2 by modified routine named `$ISAJET_LIBRARY/source/twokin.f`. The uncertainty is assigned as the maximum difference of acceptance from the nominal acceptance.

8.3.3 Parton Distribution

We calculate the uncertainty from the PDFs with the same method as that of $Z \to \tau\tau$ mentioned in Section 8.2.2.

8.3.4 Jet Energy Scale

We vary absolute and relative energy scale by 5% using JTC96X option to determine the effect on the acceptance. (EYMM,EYPP)

8.4 Summary of Systematic Uncertainties

We add in quadrature the uncertainties from each uncertainty to obtain the total systematic uncertainty. Table 14 shows the systematic uncertainty for the ratio of trigger efficiency of $Z \to \tau\tau$ to that of $\tilde{t}_1\bar{\tilde{t}}_1$ events. Table 15 and 16 show the systematic uncertainties for $Z \to \tau\tau$ and $\tilde{t}_1\bar{\tilde{t}}_1$ events, respectively.

Table 14: Systematic uncertainties for trigger efficiency from 80 to 120 GeV/c^2 .

Systematic uncertainties for trigger efficiency							(%)
$m_{\tilde{t}_1}$ (GeV/c^2)	70	80	90	100	110	120	130
Trigger efficiency	1.2	1.1	0.7	0.6	0.6	0.4	0.4

Table 15: Systematic uncertainties from $Z \to \tau\tau$ events.

Uncertainties from $Z \to \tau\tau$ (%)	
Data Stat.	17.1
PDFs	4.1
MC stat.	1.4
$\sigma_Z \cdot B(Z \to \tau\tau)$	5.2
R(0-jet)	3.1
Total	18.7

Table 16: Systematic uncertainties for the $\tilde{t}_1\bar{\tilde{t}}_1 \to b\tau^+\bar{b}\tau^- \to e\tau_h b\bar{b} + X$ events from 70 to 130 GeV/c^2 .

Systematic uncertainties for $\tilde{t}_1\bar{\tilde{t}}_1$ events							(%)
$M(\tilde{t}_1$ (GeV/c^2)	70	80	90	100	110	120	130
Gluon Radiation	4.8	5.1	5.1	4.2	3.4	3.4	3.5
Q^2 dependence	8.2	5.2	4.8	4.5	4.5	4.5	4.5
PDFs	4.6	4.7	4.5	3.9	2.5	1.7	2.0
Jet Energy Scale	3.2	3.9	2.8	1.7	1.4	1.2	1.2
MC stat.	4.7	2.9	2.4	2.0	1.9	1.6	1.7
Total	12.1	10.0	9.1	7.8	6.6	6.2	6.4

Table 17: Table of the cross section upper limit for $\tilde{t}_1\bar{\tilde{t}}_1 \to b\tau^+\bar{b}\tau^- \to e\tau_h b\bar{b} + X$ events from 70 to 130 GeV/c^2

$\tilde{t}_1$ mass	$A^{MC}_{\tilde{t}_1\bar{\tilde{t}}_1}$ (%)	$\varepsilon^{trg}_{\tilde{t}_1\bar{\tilde{t}}_1}$ (%)	Total Uncertainty (%)	$\sigma^{95\%CL}_{\tilde{t}_1\bar{\tilde{t}}_1}$ (pb)
70	0.554	77.1	22.3	36.3
80	0.932	77.5	21.2	21.1
90	1.57	77.6	20.8	12.5
100	2.06	78.1	20.3	9.4
110	2.58	78.1	19.8	7.5
120	3.08	78.5	19.7	6.2
130	3.49	78.5	19.8	5.5

9 Results

We calculate the 95% C.L. upper limits on the cross section for $\tilde{t}_1\bar{\tilde{t}}_1 \to \tau^+ b\tau^-\bar{b}$ events from $p\bar{p}$ collisions at $\sqrt{s} = 1.8$ TeV. The results are shown in Table 17 and Figure 11 for the stop masses from 70 GeV/c^2 to 130 GeV/c^2. We note that the limits are calculated using the Baysian statistics with the technique described in Ref. [36].

10 Conclusion

We have searched for the scalar top quark pair production ($\tilde{t}_1\bar{\tilde{t}}_1$) in which the $\tilde{t}_1$ decays into a tau lepton and a bottom quark via the R-parity violating process. No events were passed after the selection. We have set a 95% C.L. lower limit of the stop mass to be 110 GeV/c^2 by comparing with the NLO theoretical calculation via PROSPINO [37] with CTEQ4M.

Acknowledgments

We thank Dave Toback, Stephan Lammel, Steve Worm, Nichelle Bruner and SUSY group for providing valueable comments. We thank Bill Robertson and Dan Cronin-Hennessy for providing help for usage of VECBOS + HERWIG .

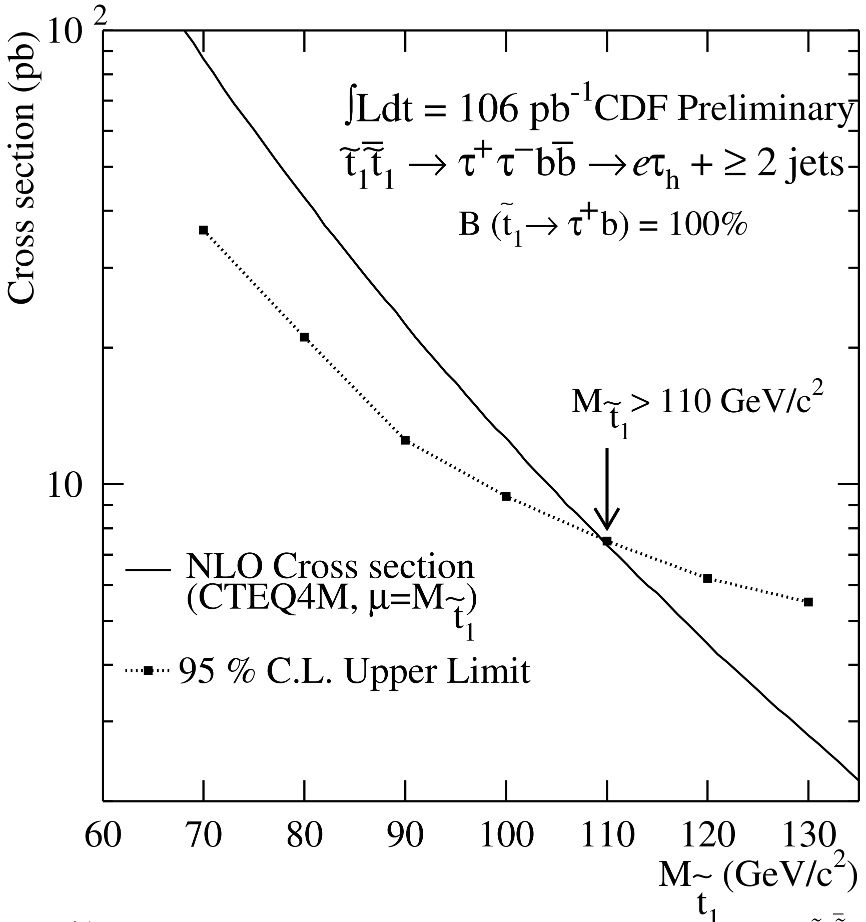

Figure 11: 95% confidence level on upper limit for cross section for $\tilde{t}_1\bar{\tilde{t}}_1 \to \tau^+ b \tau^- \bar{b}$ along with the theoretical calculation [37]

Appendix : Revised Event Selection

No candidate events pass through our selection criteria, while the expected number of background from the SM is $1.97\ ^{+1.01}_{-0.11}$ (stat) $\pm$ 0.15 (sys). In order to simplify the background estimation of vector boson events using VECBOS + HERWIG. We require $N_j \geq 2$ right after the baseline $e\tau_h$ selection followed by $M_T(e, \not{E}_T)$ and $H_T(e, \tau_h, \not{E}_T)$ cuts. The results are shown in Table18 and Figure 12. Our SM background estimation is a good agreement with data.

Cut criteria		$e\tau_h$ selection	≥ 2 jet	$M_T(e, \not{E}_T)$	$H_T(e, \tau_h, \not{E}_T)$
Z^0/γ^*+jets	OS	$140.8 \pm 0.9 \pm 7.2$	$4.9 \pm 0.1 \pm 0.4$	$4.0 \pm 0.1 \pm 0.3$	$1.67 \pm 0.09 \pm 0.14$
	LS	$0.7 \pm 0.1 \pm 0.1$	$0.0 \pm 0.0 \pm 0.0$	$0.0 \pm 0.0 \pm 0.0$	$0.00 \pm 0.00 \pm 0.00$
W+jet	OS	$76.6 \pm 3.4 \pm 4.4$	$2.7 \pm 0.2 \pm 0.2$	$0.3 \pm 0.1 \pm 0.1$	$0.14 \pm 0.04 \pm 0.01$
	LS	$22.3 \pm 1.9 \pm 1.4$	$1.2 \pm 0.3 \pm 0.1$	$0.3 \pm 0.1 \pm 0.1$	$0.03 \pm 0.01 \pm 0.01$
Diboson	OS	$1.55 \pm 0.07 \pm 0.65$	$0.22 \pm 0.02 \pm 0.09$	$0.11 \pm 0.01 \pm 0.05$	$0.06 \pm 0.01 \pm 0.02$
	LS	$0.34 \pm 0.04 \pm 0.13$	$0.12 \pm 0.02 \pm 0.05$	$0.05 \pm 0.01 \pm 0.02$	$0.01 \pm 0.01 \pm 0.01$
Top	OS	$0.73 \pm 0.09 \pm 0.19$	$0.60 \pm 0.07 \pm 0.16$	$0.10 \pm 0.03 \pm 0.03$	$0.10 \pm 0.03 \pm 0.03$
	LS	$0.10 \pm 0.04 \pm 0.13$	$0.09 \pm 0.03 \pm 0.02$	$0.00 \pm 0.00 \pm 0.00$	$0.00 \pm 0.00 \pm 0.00$
QCD	N/A	228 ± 16	6.6 ± 2.9	6.7 ± 2.6	$0\ ^{+1}_{-0}$
OS expectation		$447.2 \pm 16.3 \pm 8.6$	$15.0 \pm 2.9 \pm 0.5$	$11.2 \pm 2.6 \pm 0.3$	$1.97\ ^{+1.01}_{-0.11}\ \pm 0.15$
Data	OS	479	11	7	0
	LS	251	8	7	0

Table 18: A breakdown of the backgrounds and data as a function of event reduction requirement

.

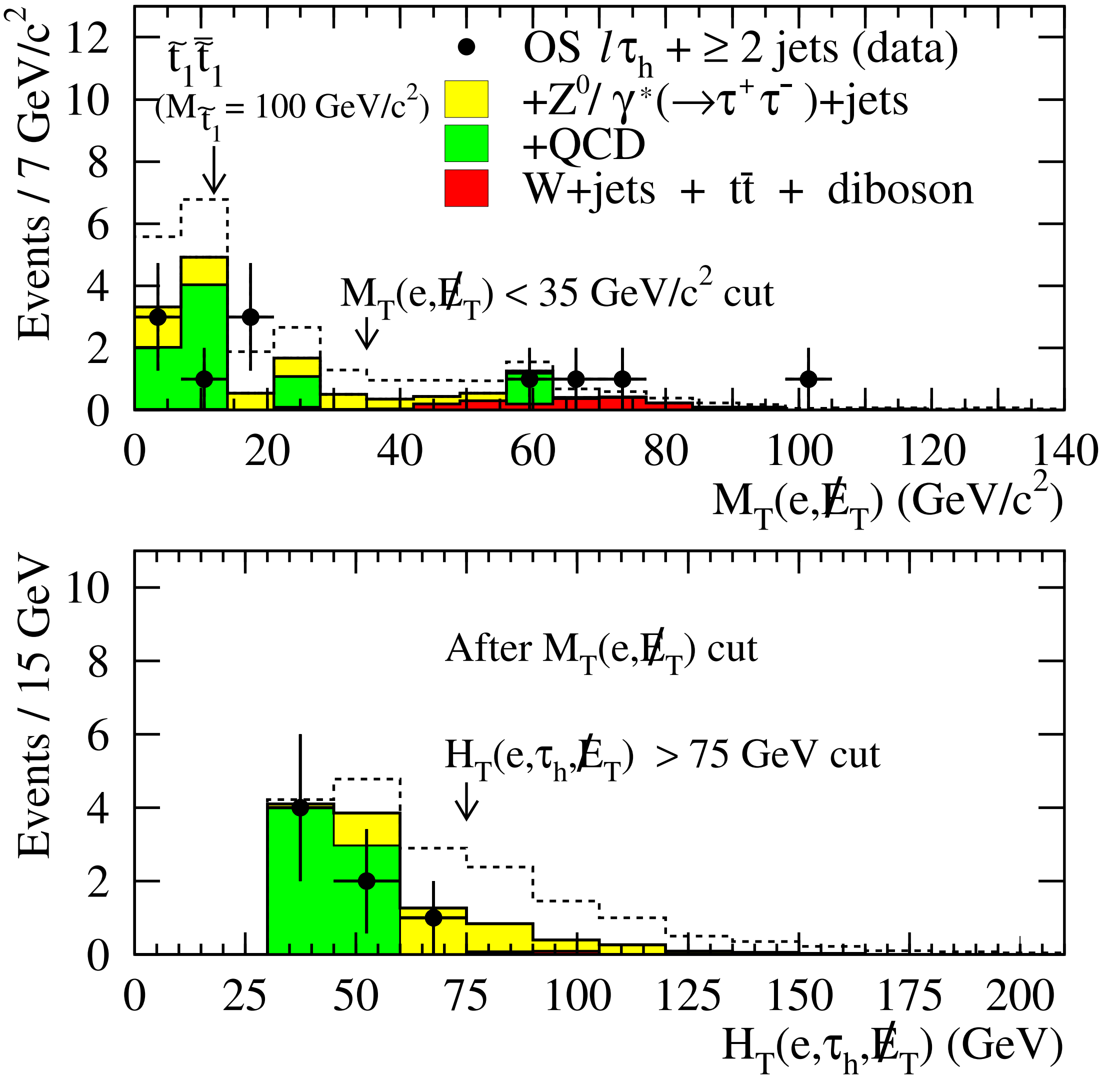

Figure 12: The data selection criteria for the opposite-sign $e\tau_h+\geq 2$ jets sample

References

[1] D. V. Volkov and V. P. Akulov, Phys. Rev. Lett. **46B**, 109 (1973); J. Wess and B. Zumino, Nucl. Phys. **B70**, 39 (1974).

[2] For reviews of the MSSM, see H. P. Nilles, Phys. Rep. **110**, 1 (1984); H. E. Haber and G. L. Kane, Phys. Rep. **117**, 75 (1985).

[3] H. Dreiner, "Introduction to Explicit R-parity Violation, hep-ph/9707435, Published in "Perspectives on supersymmetry: 462-479, " by G.L. Kane, World Scientific.

[4] Marco Aurelio Días, "The Minimal Supersymmetric Standard Model with a Bilinear R-Parity Violating Term," hep-ph/9711435 (1997), Proceedings of International Workshop On Quantum Effects In The Minimal Supersymmetric Standard Model.

[5] A. Bartl *et al.*, Phys. Lett. B **384**, 151 (1996); F. de Campos *et al.*, "R-parity Violating Decays of the Top-Quark and the Top-Squark at the Tevatron," hep-ph/9903245 (1999), Published in the proceedings of Physics at Run II: Workshop on Supersymmetry / Higgs: Summary Meeting, Batavia, IL, 19-21 Nov 1998; W. Porod, D. Restrepo, and J.W.F. Valle, "Light Stop: MSSM Versus R-parity Violation," hep-ph/0001033 (2000).

[6] ALEPH Collaboration, R. Barate *et al.*, Eur. Phys. J. C **19**, 415 (2001).

[7] Y. Miyazaki *et al.*, "Improved Extraction of $Z^0 \to \tau\tau$ Events from Low p_T Lepton Datasets in RUN IB," CDF Note 5251 (2000).q

[8] M. Gallinaro and H. Grassmann, "Observation of $Z^0 \to \tau\tau$," CDF Note 2490 (1994).

[9] T. Baumann and J. Troconiz, "Third Generation Leptoquark Search with 110 pb^{-1}," CDF Note 3840 (1996).

[10] M. Gallinaro *et al.*, "Observation of Top Dileptons with Hadronically Decaying τ Leptons," CDF Note 3461 (1996).
See /cdf/offln/cdftest/development/top/taufnd.cdf for details of the τ ID cuts.

[11] M. Hohlmann *et al.*, "A Description of the Tau-Tagging Routine TAUFND," CDF Note 2953 (1995).

[12] J.P. Done *et al.*, "Study of Run-1B Lepton Identification Efficiencies for SUSY Searches," CDF Note 4218 (1997).

[13] J.P. Done *et al.*, "Study of Run-1B Lepton Isolation Efficiencies for SUSY Searches," CDF Note 4291 (1997).

[14] K. Byrum *et al.*, "The Level-2 Trigger Efficiency for 9 GeV Electrons in Run IA - Part II," CDF Note 3665 (1998).

[15] T. Kamon *et al.*, "Study of the Inclusive Lepton Trigger Efficiency for the Run IA SUSY Trilepton Analysis," CDF Note 2596 (1998).

[16] W. Taylor *et al.*, "Run 1B Level 2 CEM_8_CFT_7_5 and XCES Electron Trigger Efficiencies," CDF Note 4691 (1998).

[17] N.L. Bruner, "Level 3 Trigger Efficiencies for the Low p_T Inclusive Lepton Data Sets MULB and ECLB," CDF Note 4700 (1998).

[18] K. Byrum, "Luminosity for Run IB Inclusive Electron Binary Dataset," CDF Note 5001 (1999).

[19] Top Group, "Sample Selection for Run 1B Top Search," CDF Note 2966 (1995).

[20] H. L. Lai, J. Huston, S. Kuhlmann, F. Olness, J. Owens, D. Soper, W. K. Tung, and H. Weerts, "Improved parton distributions from global analysis of recent deep inelastic scattering and inclusive jet data", Phys. Rev. D **55**, 1280 (1997).

[21] H. Baer, F.E. Paige, S.D. Protopopescu, and X. Tata, hep-ph/0001086. We use version 7.44.

[22] J.P. Done *et al.*, "ISAJET Monte Carlo Validation," CDF Note 4903 (1999).

[23] D. Cronin-Hennerssy *et al.*, "Measurement of the $W^{\pm} \to e^{\pm}+$ n Jet Cross Section in 1.8 TeV $p\bar{p}$ Collisions," CDF Note 3070 (1996).

[24] C. Loomis, "Using TAUOLA, A Decay Library for Polarized τ Leptons," CDF Note 2796 (1994).

[25] J.D. Lewis and P. Avery, "CLEOMC: The CDF Interface to the CLEO Monte Carlo (QQ)," CDF Note 2724 (1994).

[26] CDF Collaboration, F. Abe *et al.*, Phys. Rev. D **76**, 3070 (1996).

[27] CDF Collaboration, F. Abe *et al.*, Phys. Rev. D **49**, 1 (1994).

[28] Top Group, "The New CDF Run 1 Combined t-tbar Production Cross Section," CDF Note 5043 (1999).

[29] CDF Collaboration, F. Abe *et al.*, Phys. Rev. Lett. **78**, 4536 (1997).

[30] J. Ohnemus, Phys. Rev. D **44**, 3477 (1991).

[31] J. Ohnemus and J. Owens, Phys. Rev. D **43**, 3626 (1991).

[32] D. Cronin-Hennerssy *et al.*, "Measurement of the $Z \to e^+e^-+$ n Jet Cross Section in 1.8 TeV $p\bar{p}$ Collisions, " CDF Note 3360 (1996).

[33] M. Glück, E. Reya, and A. Vogt, Z. Phys. C **69**, 433 (1995).

[34] A. D. Martin, R. G. Roberts, W. J. Stirling, Phys. Lett. B **387**, 419 (1996).

[35] CDF collaboration, F. Abe *et al.*, Phys. Rev. Lett. **76**, 3070 (1996).

[36] John Conway *et al.*, “Upper Limits on Poisson Processes Incorporating Uncertainties in Acceptance and Background,” CDF Note 4476 (1996).

[37] W. Beenakker *et al.*, “PROSPINO : A Program for the Production of Supersymmetric Particles in Next-to-Leading Order QCD”, hep-ph/9611232 (1996).